Journal of The
Electrochemical Society

Electrolyte Compatible Separator Materials for Sodium-Ion Battery

Journal of The Electrochemical Society, 2025 **172** 060515

Electrolyte Compatible Separator Materials for Sodium-Ion Battery

Owen S. Wostoupal,[1,2] Xiaowei Wang,[1] Qian Liu,[1] Tao Xu,[2] and Zhengcheng Zhang[1,3,z]

[1]*Chemical Sciences and Engineering Division, Argonne National Laboratory, Lemont, Illinois 60439, United States of America*
[2]*Department of Chemistry and Biochemistry, Northern Illinois University, DeKalb, Illinois 60115, United States of America*
[3]*Pritzker School of Molecular Engineering, The University of Chicago, Chicago, Illinois 60637, United States of America*

Sodium-ion batteries (NIBs) have emerged as an alternative electrochemical energy storage to replace lithium-ion batteries (LIBs). Separator is one of the key components that dictates the cell performance of NIB. Significant progress has been made in electrolyte research, however for most cases glass fiber has been used as separator due to its remarkable electrolyte wettability despite its many disadvantages. In this study, we evaluated commercially available porous materials as separator material for NIB. Porous polyvinylidene fluoride (PVDF) membrane stands out as a universal separator which exhibits high compatibility with a wide range of electrolytes and electrodes and demonstrates high electrochemical stability evaluated in hard carbon/Na half cells and $NaNi_{1/3}Fe_{1/3}Mn_{1/3}O_2$ (NFM111)/hard carbon full cells. This research highlights the PVDF membrane as a viable separator for advancing NIB research, enabling the development of new electrolyte materials without the separator constraints of wetting limitations or excessive electrolyte consumption.

 [DOI: 10.1149/1945-7111/addef1]

Manuscript submitted April 4, 2025; revised manuscript received May 5, 2025. Published June 12, 2025.

Supplementary material for this article is available online

Sodium-ion batteries (NIBs) have attracted significant attention due to higher abundance and availability of sodium in the Earth's crust, making NIBs a more cost-effective alternative to lithium-ion battery (LIB).[1] Additionally, NIBs offer an improved temperature range, allowing them to function more effectively under extreme conditions.[2] While LIBs perform optimally within a narrow temperature range of 15 °C–35 °C, their performance deteriorates significantly at extreme temperatures.[3] Besides, NIBs have demonstrated faster charging capabilities at higher rates compared to LIBs leveraging on the faster kinetics of Na^+ storage in hard carbon (HC) anodes.[4] Notably, as NIBs utilize an aluminum current collector at anode, they can be fully discharged and stored at zero volts.[5] This simplifies the transportation of NIBs and reduces the risk of thermal runaway.[6] Upon these factors, NIBs can outperform over lithium-ion counterparts. Despite their merits, NIBs currently face a key limitation: their lower energy density compared to LIBs. This disparity is due to the standard redox potential of Na^+/Na is −2.7 V (vs standard hydrogen electrode, SHE), which is less negative than that of Li^+/Li (−3.04 V, vs SHE), resulting in less energy stored per unit charge.[7–9] This indicates higher-voltage cathode materials with higher specific capacity for NIBs are needed to achieve compatible energy density to LIBs. However, it triggers more severe parasitic reactions with electrolytes due to expanded voltage range. To mitigate this drawback, extensive research and development has been employed for high-voltage stable electrolytes.[10–15]

Although research on improving the performance of NIBs has advanced significantly, particularly in the development of cathodes[16–19] and anodes,[20–23] studies on separators remain limited. Separators are critical components in NIBs, as they directly impact electrochemical performance, safety, and the compatibility between the electrolytes and electrodes. An effective separator not only ensures the separation of the positive and negative electrodes but absorbs sufficient electrolyte to facilitate Na^+ ion transport. For LIB applications, commonly used separators are polyolefin thermoplastics like polypropylene (PP) and polyethylene (PE).[24] Polyolefin separators offer improved mechanical strength, which helps prevent dendrite penetration, and do not require excess electrolyte volume to achieve good electrochemical performance.[25] However, they have limited wettability with conventional carbonate-based electrolytes dissolved with sodium salt for NIBs, resulting in a high contact angle due to the hydrophobic nature of the separator surface.[26] This wetting incompatibility with various electrolytes hinders the separator's performance in electrochemical testing, as premature cell shorting has been reported due to poor wetting and higher resistance.[27] New non-carbonate electrolytes have the same wettability issue which has impeded the development progress. To solve the above issue, a porous and thick glass fiber (GF/C) separator is commonly used and reported for NIB research.[28–30]

GF/C separator has been proven to be an effective separator due to its high porosity, high electrolyte wettability, and high ionic conductivity.[31,32] Notably, GF/C can wet most solvents, including carbonates, esters, ethers, ionic liquids, and many others, demonstrating excellent compatibility with various solvent systems. These attributes enable its popular use for the further development of electrolytes in NIBs. However, GF/C has limitations, such as high porosity, low mechanical strength, significant thickness (>260 μm), and poor workability.[33] The high thickness results in excessive electrolyte uptake, leading to the consumption of large amounts of electrolyte. Reports also indicate that the practical application of GF/C is compromised in NIBs due to sodium dendrite formation, growth, penetration and electrical circuit shorting.[34,35]

Numerous research efforts have been devoted to developing advanced electrolyte systems in combination with compatible separators for NIBs. Some included direct use of gel polymer electrolytes (GPE) as separators and some introduced a GPE coating on conventional separators like GF/C to improve the mechanical strength,[32,36] and other compositions through an electrospinning method for a nanofiber electroactive β-phase separator with or without coating another polymer material.[37–39] Still, GPE is mechanically weak and the GPE coating on materials like GF/C, PP, etc makes the separator fabrication exhausting. Among GPEs, poly (vinylidene fluoride-co-hexafluoropropylene) (PVDF-HFP)-based gel polymer electrolytes have been typically prepared using various solvents. However, PVDF-HFP lacks good ionic conductivity itself, undergoes thermal shrinkage, and has poor mechanical strength.[40] To efficiently advance the electrolyte frontier, a highly wettable separator must be identified that can deliver consistent electrochemical performance without negatively impacting the results.

[z]E-mail: zzhang@anl.gov

In this study, a commercially available porous polyvinylidene fluoride (PVDF) membrane was investigated as a separator for NIBs. As a result, the chemical properties of PVDF enable a lower electrolyte contact angle of close to 0°, enhancing electrolyte wettability and facilitating the absorption of various solvents, thus mitigating compatibility issues with electrolyte formulations in NIBs. Furthermore, PVDF offers sufficient mechanical strength, and its comparatively smaller thickness ensures reasonable electrolyte uptake. In HC/Na half-cell tests, the PVDF separator significantly improved anode capacity at varying rates. In full-cell configurations based on HC anode and $NaNi_{1/3}Fe_{1/3}Mn_{1/3}O_2$ (NFM111) cathode, it demonstrated a capacity retention of 70.1% over 200 cycles with high Coulombic efficiency. These results highlight the high stability and compatibility of PVDF separators presenting stable electrochemical performance, which lays a foundation for advanced electrolyte studies for NIBs.

Experimental

Materials.—The chemicals used for the electrolyte formulation included sodium hexafluorophosphate ($NaPF_6$, American Elements), ethylene carbonate (EC, Gotion), dimethyl carbonate (DMC, Sigma-Aldrich), ethyl methyl carbonate (EMC, Gotion), fluoroethylene carbonate (FEC, Sigma-Aldrich). The chemicals used for the wetting test of the separators include ethyl methyl carbonate (EMC), dimethyl carbonate (DMC), propylene carbonate (PC, Sigma-Aldrich), 1,3-dioxolane (DOL, Sigma-Aldrich), diethyl carbonate (DEC, Gotion), fluoroethylene carbonate (FEC), acetonitrile (AN, Sigma-Aldrich), *N*-propyl-*N*-methylpyrrolidinium bis(fluorosulfonyl)imide (PMpyrFSI, Solvionic), 2H-tetrafluoroethyl 2,2,3,3-tetrafluoropropyl ether (TTE, Apollo Scientific), dimethyl sulfoxide (DMSO, Sigma-Aldrich), diethylene glycol dimethyl ether (DEGDME, TCI America), dimethyl ether (DME, Sigma-Aldrich), tetrahydrofuran (THF, Sigma-Aldrich), and trimethyl phosphate (TMP, Sigma-Aldrich). The chemicals used for the preparing the hard carbon laminates (Fig. S4a) included hard carbon powder (MTI Corporation), super C45 carbon black (Timcal), N-methylpyrrolidone (NMP, Sigma-Aldrich), and 8% polyvinylidene fluoride in NMP (APV Engineered Coatings). The commercially available separators included glass fiber (GF/C, Whatmann, Cytiva 1822–125), polyvinylidene fluoride membrane (PVDF, Durapore, Sigma-Aldrich VVLP04700), trilayer polypropylene-polyethylene-polypropylene (PP/PE/PP) membrane (C2325, Celgard), and monolayer surfactant-coated polypropylene (PP) membrane (C3401, Celgard).

Characterization.—The surface and cross-sectional morphology of the separators, as well as the surface of the HC and NFM111 electrodes, were examined using a scanning electron microscope (SEM, Hitachi S-4700-II CFE-SEM with EDS). The working distance was 13–14 mm, and the accelerating voltage was 5.0 kV. The mechanical strength properties including the tensile strength and Young's modulus were obtained by using a universal tensile strength tester (Instron 3300 Series universal Testing System) with a stretching rate of 5 mm s^{-1}. Separator dimensions were fixed at 4.0 cm × 1.0 cm. The electrolyte uptake measurements were investigated by immersing the separators in 1.0 ml of the 1.0 M $NaPF_6$ in EC/EMC/DMC 1/1/1 by volume with 5 wt% FEC electrolyte solution for 8 h. The absolute mass of the electrolyte and electrolyte uptake percentage was calculated by using Eq. 1:[41]

$$\text{Electrolyte Uptake}(\%) = \frac{(M - M_o)}{M_o} \times 100\% \quad [1]$$

where M_o is the mass of the separator and M is the mass of the electrolyte-soaked separator.

The contact angle measurements were investigated using a contact angle meter (CAM-plus). The volume of electrolyte dropped on the separator's surface was fixed at 20 μl. Images were taken a couple of seconds after the electrolyte was dropped on that surface and the contact angle line was adjusted on the display window. The contact angle was calculated using 2θ with the angle observed by aligning the display line towards the apex of the droplet on the separator surface.[42]

Electrochemical Measurements

Electrical impedance spectroscopy (EIS) was accomplished using an electrochemical workstation (Solartron Analytical 1470E Cell Test System) in order to obtain the ionic conductivities and activation energies of the separators. Symmetric cells were tested composed of stainless steel||separator||stainless steel between 100 kHz to 0.1 Hz. The ionic conductivities were calculated using Eq. 2:[43]

$$\sigma = \frac{l}{R_b \times A} \quad [2]$$

where R_b is the bulk resistance, l is the thickness of the separator, A denotes the contact area between the separator and the electrodes, and σ is the ionic conductivity.

Linear sweep voltammetry (LSV) was achieved through an electrochemical workstation (Solartron Analytical 1470E Cell Test System) with cells comprised of Na-metal||separator||aluminum foil and Na-metal||separator||stainless steel. The test protocol was set from open current voltage to 5.0 V (vs Na^+/Na) with a scan rate of 1.0 mV s^{-1}.

The rate test for the HC/Na half cells was charged and discharged with different rates from 0.02 C to 1 C (1 C = 300 mA g^{-1}) with the voltage range of 0.01 V to 2.0 V. The NFM111/HC full cell electrochemical performance was evaluated after formation (0.1 C) with C/3 with a cutoff voltage of 1.0 V–4.15 V. All tests were conducted at 30 °C in a battery cycler (Neware Technology).

Results and Discussion

Physical properties of separators.—Table I summarizes the specification and physical properties of GF/C, PVDF, C2325, and C3401 separators including their composition, pore size (μm), porosity (%), and thickness (μm). GF/C exhibits significantly larger pore size a few magnitudes higher than other separators and this infinitely high porosity yields no barrier of electrolyte absorption and ion transport in NIBs. Specifically, GF/C has a fibrous structure with fiber widths ranging from 0.25 to 1.5 μm, contributing to its large pore size and exceptionally high porosity (Fig. 1). PVDF, C2325, and C3401 separators exhibit microporous structures with notable differences in pore size and porosity. PVDF has a pore size of 0.1 μm, which is over twice as large as C3401 (0.043 μm) and more than three times larger than C2325 (0.028 μm). In addition to its

Table I. Physical properties of GF/C, PVDF, C2325, and C3401 separator.

Separator	Composition	Pore size (μm)	Porosity (%)	Thickness (μm)
GF/C	Borosilicate Glass	1.2	80–85	260
PVDF	Hydrophilic PVDF Membrane	0.1	70	125
C2325	Trilayer microporous membrane (PP/PE/PP)	0.028	39	25
C3401	Surfactant coated monolayer microporous membrane (PP)	0.043	41	25

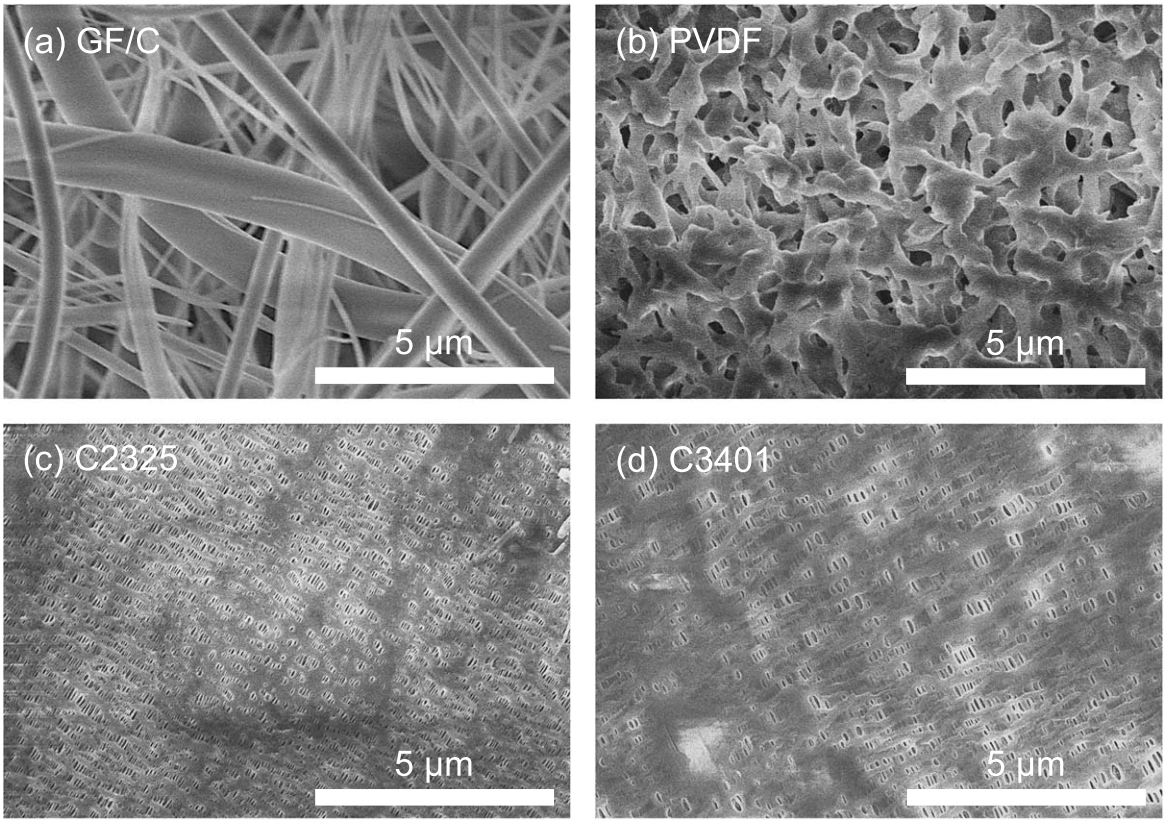

Figure 1. SEM images of the surface morphology for (a) GF/C, (b) PVDF, (c) C2325, and d) C3401 separator.

larger pore size, PVDF's 70% porosity can enhance electrolyte absorption without possibly impeding ion flow. Although GF/C's high porosity allows it to easily absorb electrolyte, its substantial thickness (260 μm) necessitates a larger electrolyte amount to fully wet the separator. In contrast, PVDF has a reduced thickness of 125 μm, making it a more suitable choice for minimizing electrolyte volume during cell assembly. Despite the lowest thickness (25 μm) and porosity (35%–40%), both C2325 and C3401 separators suffer from sufficient electrolyte wetting issue and concludes as unsuitable separators for NIB research.

Electrolyte Wettability of Separators

Unlike GF/C, most battery separators are composed of high molecular weight polymers, and their chemical and physical properties are highly dependent on the polymeric backbones and microporous structure. Figure 2 shows the chemical structure of polyolefin-based separators.[44–46] The fluorination in PVDF backbone, compared to the hydrocarbon chains in PE and PP, alters its dielectric constant, polarity, mechanical and thermal stability.[47,48] Additionally, electrolyte affinity can be distinguished based on the polymer backbone. As reported by Changzhen et al., hydrocarbon polymers exhibit low dipole moments, limited electronegativity, and low surface energy. As a result, they demonstrate poor wettability toward electrolyte solvents with high dielectric constants, such as DMC, PC, and EC.[49] In contrast, due to the stronger polarity and higher electronegativity arising from the C–F bond, the PVDF separator can readily absorb polar electrolytes.[50,51]

To further evaluate its electrolyte wettability, PVDF membrane was tested with various electrolyte solvents that could be potentially used in NIB and the results are compared with GF/C, C2325 (a trilayer PP/PE/PP membrane), and C3401 (a surfactant-coated monolayer PP membrane) (Fig. 3). When 50 μl of electrolyte solvent was applied to the surface of the separator, PVDF and GF/C exhibited simultaneous wetting behavior for all the solvents. Due to the high porosity of GF/C, each solvent is easily absorbed, while

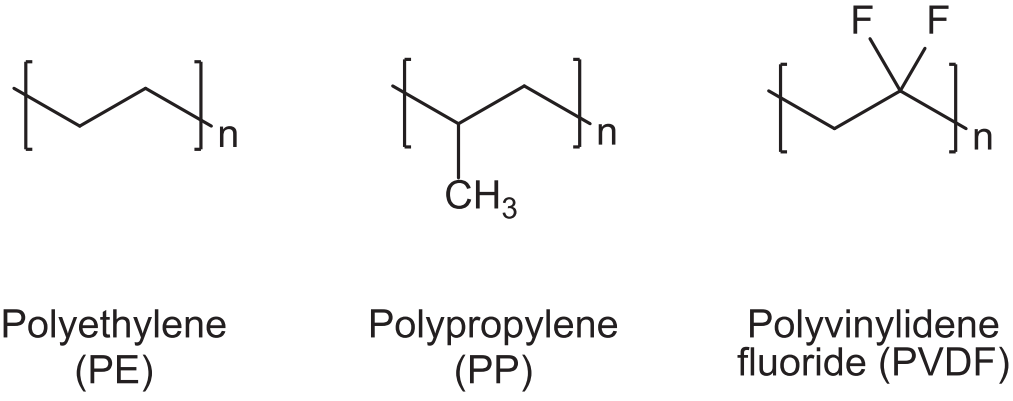

Figure 2. Molecular structures of polyethylene (PE), polypropylene (PP), and polyvinylidene fluoride (PVDF) materials.

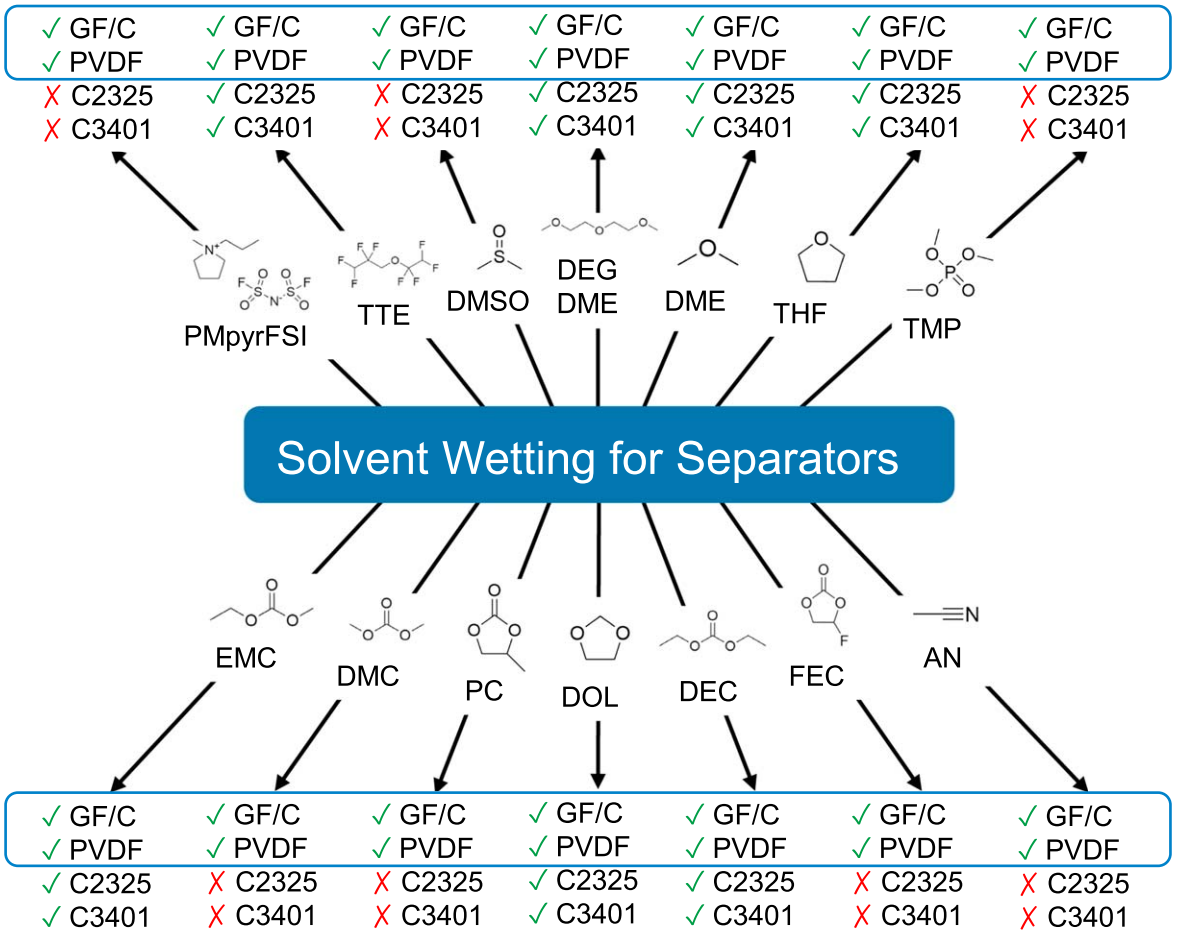

Figure 3. Schematic of wetting capability for the GF/C, PVDF, C2325, and C3401 separators using various electrolyte solvents.

the wettability of other separators is limited by surface tension resulting from their lower porosity. Remarkably, the solvent wettability of the PVDF is broader, likely due to the fluorinated backbone structure and higher porosity. In contrast, separator C2325 exhibited non- wetting behavior with solvents such as DMC, PC, FEC, AN, DMSO, TMP and PMpyrFSI (Fig. S1). The surfactant-coated separator C3401 allowed slightly higher absorption of these solvents, but the underlying PP membrane remained resistant. This pronounced difference in electrolyte wetting highlights the advantages of GF/C and PVDF separators for screening various solvent systems, as their enhanced wettability minimizes the risk of separator-induced performance limitations.

The electrolyte contact angle of the separator was evaluated by depositing a quantified amount (50 μl) conventional electrolyte of

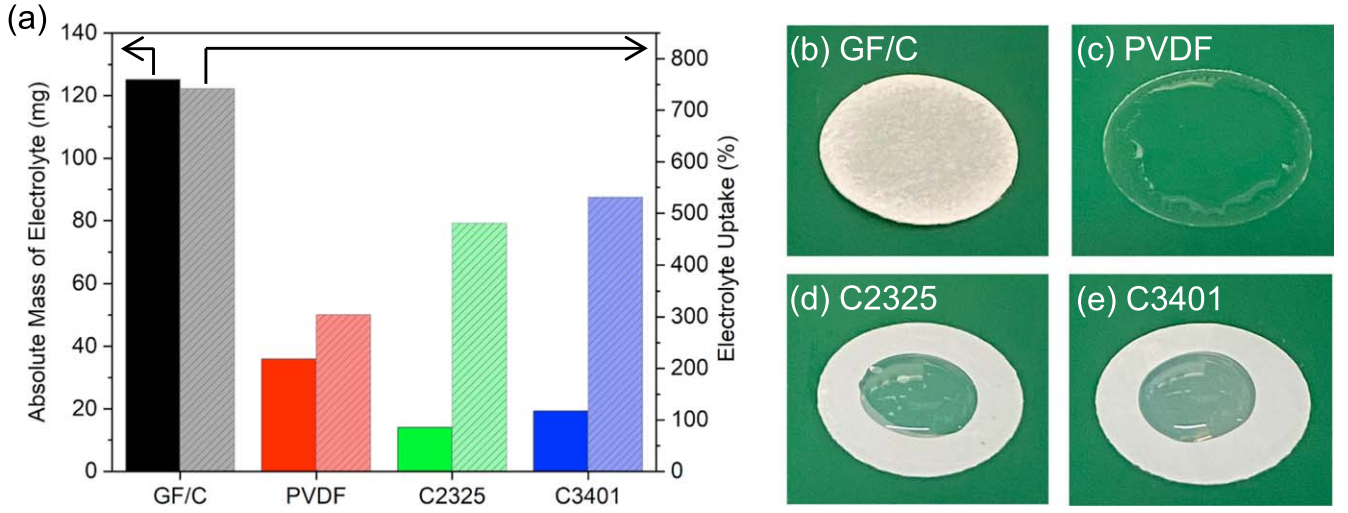

Figure 4. Separator wettability with baseline electrolyte. (a) Electrolyte uptake of the GF/C, PVDF, C2325, and C3401 separators. The solid bar indicates the absolute mass of electrolyte (mg) that can be absorbed by the separator. The shaded bar indicates the electrolyte uptake (%), which can be calculated using Eq. 1. Images of 50 μl of the electrolyte added onto each of the (b) GF/C, (c) PVDF, (d) C2325, and (e) C3401 separators.

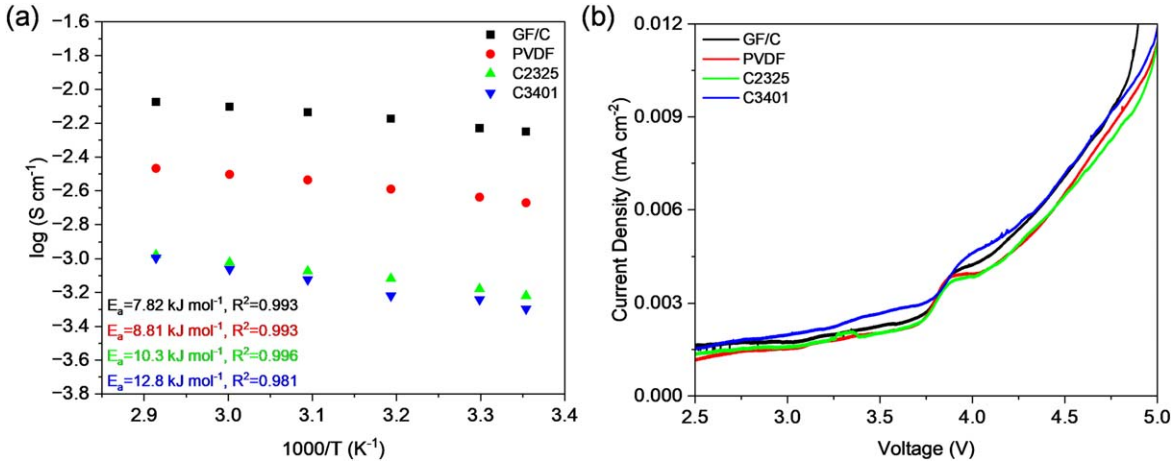

Figure 5. (a) Ionic conductivity and activation energies (E_a) of the GF/C, PVDF, C2325, and C3401 separators. (b) LSV profiles of GF/C, PVDF, C2325, and C3401 separators.

1.0 M $NaPF_6$ in EC/EMC/DMC (1/1/1 by volume) + 5 wt% FEC onto the separator surface. Similar to the pure solvent wetting analysis, GF/C and PVDF readily absorbed the electrolyte solution (Figs. 4b and 4c). However, the edges of GF/C remained dry due to its exceptionally high electrolyte uptake. In contrast, C2325 and C3401 exhibited poor wettability, as evidenced by their significantly higher contact angles (Figs. 4d–4e). Specifically, the contact angle for C2325 was 74°, and for C3401, it was 70° when same amount of electrolyte was applied to the separator surface (Figs. S5c–S5d). GF/C and PVDF showed no measurable contact angle, indicating excellent wettability (Figs. S5a–S5b). With the exceptional wetting properties of GF/C and PVDF, separator-induced performance limitations from wetting of electrolyte are unlikely for these materials.

The electrolyte uptake is a critical parameter, as insufficient wetting of the separator can compromise battery cell performance.[52] Electrolyte uptake refers to the volume of electrolyte required to fully saturate the separators. After soaking the separators in baseline electrolyte, the absolute mass of electrolyte retained within each separator was measured. GF/C exhibited a significant increase in both the absolute mass of electrolyte retained within the separator and electrolyte uptake (Fig. 4a). This behavior can be attributed to its high porosity, substantial thickness, and excellent wettability, which enable it to absorb the electrolyte effectively, like a sponge. In contrast, PVDF exhibited a lower absolute mass of electrolyte within the separator, primarily due to its significantly lower porosity and thickness compared to GF/C. Similarly, the thickness and porosity of C2325 and C3401 are considerably lower than those of GF/C and slightly lower than those of PVDF, resulting in a reduced absolute mass of electrolyte retained within these separators. The PVDF separator, with a larger mass (17.6 mg) compared to C2325 (3.7 mg) and C3401 (4.5 mg), exhibits lower electrolyte uptake due to the reduced electrolyte mass relative to the separator mass. The increased wettability of PVDF enables it to achieve lower electrolyte uptake, thereby reducing electrolyte usage in relation to the separator mass.

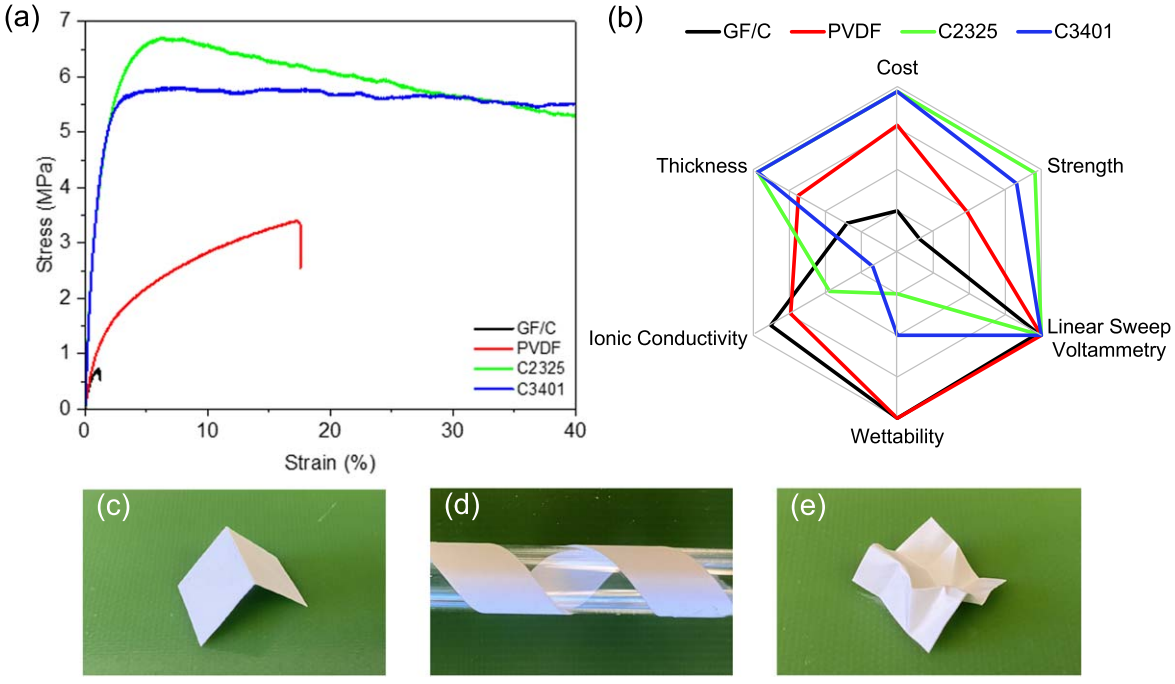

Figure 6. (a) Tensile strength of GF/C, PVDF, C2325, and C3401 separators. (b) Radar chart for properties of GF/C, PVDF, C2325, and C3401 separators. The parameters include cost (inverse of separator purchase cost), strength (stress resistance before tearing), LSV (electrochemical stability reflected by the decomposition voltage), wettability (wetting compatibility with pure solvents), ionic conductivity (separator-induced resistance), and thickness (inverse of separator thickness). Workability of PVDF separator - (c) folding, (d) twisting, and (e) crumpling.

Ionic Conductivity and Electrochemical Stability

Ionic conductivity measurements were conducted to assess the kinetics and resistance associated with each separator by assembling stainless steel||separators||stainless steel symmetrical cells. All the symmetrical cells assembled used 100 μl of baseline electrolyte 1.0 M $NaPF_6$ in an EC/EMC/DMC (1/1/1 by volume) + 5 wt% FEC. High separator resistance indicates poor Na^+ ion transport kinetics. As shown in Fig. 5a, the large pore size and high porosity of GF/C contribute to its superior ionic conductivity, resulting in lower resistance. PVDF exhibits slightly lower ionic conductivity than GF/C, which can be attributed to its smaller pore size and reduced porosity. However, the exceptional wettability of PVDF enhances its ionic conductivity despite having lower electrolyte uptake compared to C2325 and C3401. In contrast, C2325 and C3401 demonstrate poor ionic conductivities, primarily due to their smaller pore sizes and limited electrolyte wettability.

The electrochemical window of the separators was evaluated by linear sweep voltammetry (LSV) (Fig. 5b). Aluminum foil was used as working electrode and Na metal as reference and counter electrodes at a sweep scan rate of 1 mV s^{-1}. All separators exhibited nearly identical LSV profiles when the voltage increased from the open-circuit voltage to 5.0 V vs Na^+/Na, suggesting the separators play a minimal role during the LSV, as the primary contribution, particularly at voltages below 5.0 V, arises from electrolyte decomposition. The slope observed at 3.75 V in the LSV curves can be attributed to the oxidation of the baseline electrolyte, a trend consistent across all separators evaluated.

Mechanical Strength of Separators

The tensile strength of separators is a critical property for battery cells, as a robust separator can resist tears or punctures caused by sodium metal dendrites. GF/C was found to be brittle, tearing at a strain of less than 2% (Fig. 6a). This poor mechanical strength is attributed to its composition of inorganic borosilicate glass fibers and its large pore size.[53] Although GF/C is thicker than other separators, its structure unravels easily and tears under minimal stress, making it inadequate for practical applications. In contrast, PVDF demonstrated improved mechanical strength, withstanding up to 17% strain before tearing. This enhanced tensile strength allows PVDF to endure various operating conditions without mechanical failure, improving its suitability for use in NIB and sodium metal batteries (Figs. 6c–6e). C2325 and C3401 exhibit enhanced mechanical strength compared to GF/C and PVDF. These separators can withstand over 40% strain with C2325 reaching a stress limit of 6.68 MPa at 6.71% strain and C3401 achieving 5.76 MPa at 7.49% strain. Additionally, the Young's modulus value for PVDF is 93.2 MPa, 328.8 MPa for C2325, and 402.4 MPa for C3401 whereas no such value is obtained for GF/C due to its immediate tearing during testing. These results demonstrate that C2325 and C3401 can effectively stretch and deform under stress, which enhances their ability to resist dendrite punctures. This deformation capability is critical for preventing dendrite-induced short circuits in battery cells.[35] Although the mechanical strength of C2325 and C3401 is significantly improved, their electrolyte wetting limitations still make them unsuitable for electrolyte development in NIBs.

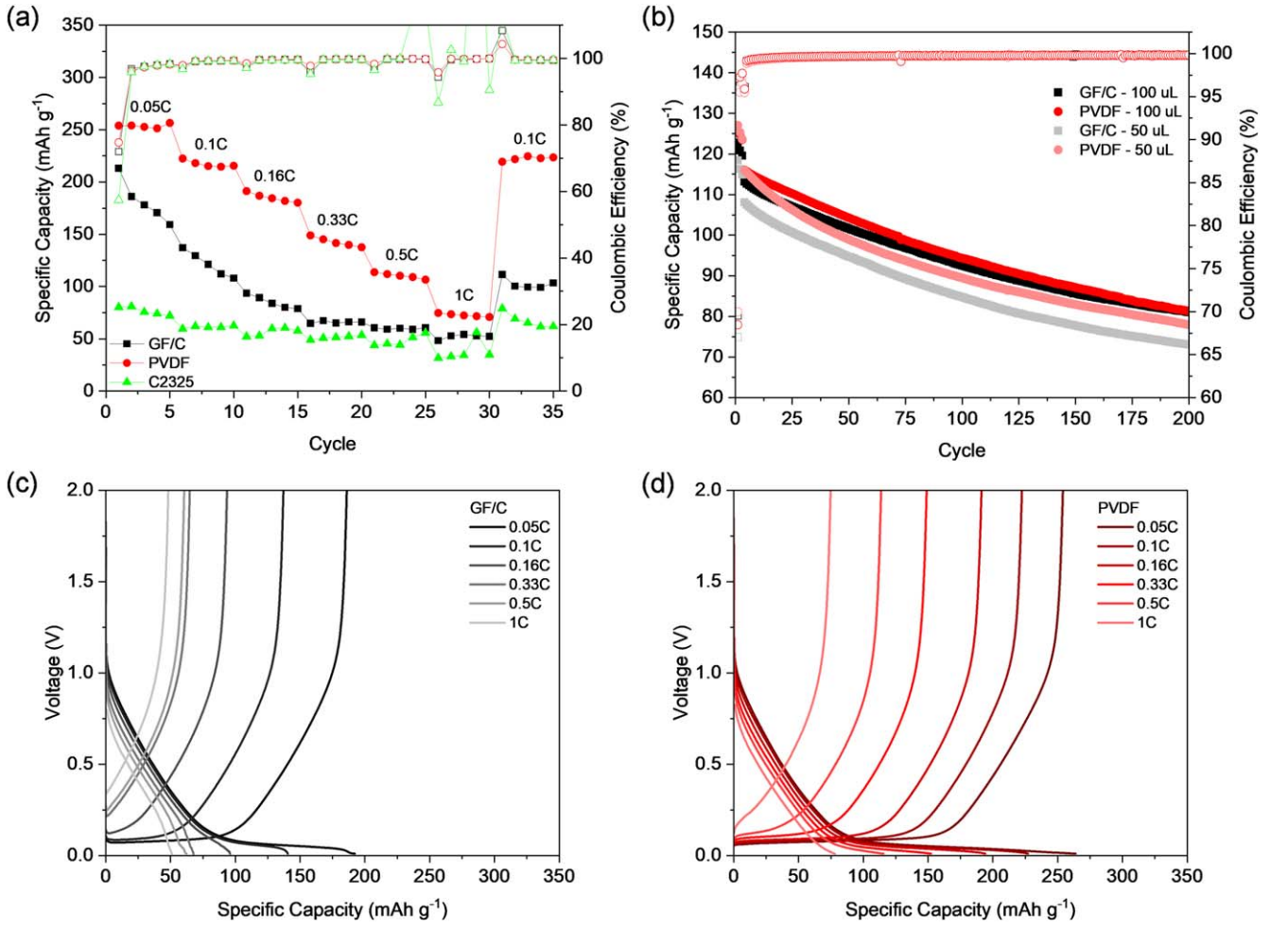

Figure 7. Electrochemical performance of separators. (a) C-rate performance of GF/C, PVDF, and C2325 in HC/Na cells (100 μl of electrolyte with a cutoff voltage of 0.01–2.0 V), (b) cycling performance of the GF/C and PVDF separators in NFM111/HC full cells (50 μl and 100 μl of baseline electrolyte with a cutoff voltage of 1.0–4.15 V). Voltage profiles of the second cycle at 0.05 C and first cycle at all other C-rates for (c) GF/C separator and (d) PVDF separator in HC/Na half cells.

NIB Cell Performance of Separators

The electrochemical performance of the separators was evaluated in HC/Na half cells with 100 μl of baseline electrolyte 1.0 M $NaPF_6$ in an EC/EMC/DMC (1/1/1 by volume) + 5 wt% FEC. At lower rates (0.05 C, 0.1 C, and 0.16 C), significant differences were observed between separators. PVDF exhibited the highest capacity and stability, whereas GF/C showed rapid capacity decay, and C2325 displayed low initial Coulombic efficiency, resulting in significantly reduced capacity. PVDF has tremendous value for allowing sufficient electrolyte absorption facilitating an increased electrochemical stability (Fig. 7a). The instability of GF/C can be attributed to its high electrolyte demand, which resulted in the incomplete wetting of the separator compromising its performance. C2325 demonstrated high resistance and poor wettability for Na^+ ion kinetics in the electrolyte, consistent with previous findings, explaining its poor cell performance. Furthermore, C3401 exhibited an even lower ionic conductivity than C2325, resulting in a short circuit after the first cycle of the rate performance test (Fig. S9).

At higher rates (0.33 C, 0.5 C, and 1 C), the capacity difference between GF/C and C2325 narrowed due to significant sodium inventory loss in GF/C during cycling. PVDF demonstrated high capacity and stability at elevated rates, which can be attributed to its excellent wetting properties and lower electrolyte uptake. These characteristics enable better performance under such conditions. The primary distinction between PVDF and GF/C separators lies in the intercalation plateau capacity at lower and higher rates (Figs. 7c and 7d). For sodium-ion storage within HC, approximately half of the capacity is derived from adsorption, while the other half arises from intercalation.[54] At each rate from 0.05 C to 1 C, the intercalation capacity of GF/C was severely compromised, thereby limiting the overall capacity. This substantial capacity loss may result from electrolyte consumption by Na metal due to the formation of an unstable solid electrolyte interphase, thereby impairing the electrochemical performance of GF/C, particularly since it requires a larger electrolyte volume due to its high electrolyte uptake.[55] In contrast, the PVDF separator demonstrates improved performance, maintaining comparable adsorption capacities and achieving higher intercalation capacities than GF/C.

NFM111 (Fig. S4b) /HC full cells were finally evaluated using baseline electrolyte with two different amounts. With a 100 μl electrolyte addition, both GF/C and PVDF exhibited similar performance in terms of capacity retention and Coulombic efficiency during formation and higher-rate cycling. However, when the electrolyte volume was reduced to 50 μl, a noticeable capacity difference emerged, even at low C-rate formation cycles (Fig. 7b). After the first formation cycle, the Coulombic efficiency of GF/C was 67.0%, compared to 70.0% for PVDF. The high electrolyte uptake of GF/C began to inhibit the battery's performance at this reduced electrolyte volume, whereas PVDF maintained performance comparable to that observed with 100 μl electrolyte. Following the initial formation cycle, PVDF demonstrated similar Coulombic efficiency and cycling stability to GF/C but sustained a higher capacity, thereby exhibiting better overall performance. The excellent wettability and low electrolyte uptake of PVDF enable it to perform efficiently even with lean electrolyte volumes.

Conclusions

A systematic study of commercially available separator materials has been performed to address the issue of electrolyte wettability in NIB. Among the screened separators, porous PVDF membrane stands out as an alternative separator to GF/C glass fiber for NIB due to its optimal properties in polarity, electrolyte wettability, mechanical strength and electrochemical performance. These properties enable consistent cell performance in NIB research, supporting the advancement of new electrolytes and electrodes design and development without interference from the separator materials.

Acknowledgments

This work was funded by the U.S. Department of Energy (DOE), Office of Energy Efficiency and Renewable Energy, Vehicle Technologies Office. The submitted manuscript has been created by UChicago Argonne, LLC, Operator of Argonne National Laboratory, which is supported by DOE Office of Science under Contract No. DE-AC02–06CH11357. Z.Z. and X.W. conceived the idea. O.W. and Q.L. designed the experiments. Z.Z. and T.X. initiated and supervised the project. O.W. and X.W. wrote the manuscript with input from all authors. All authors discussed the results, co-wrote, and commented on the manuscript. All the authors declare no competing interests.

ORCID

Owen S. Wostoupal https://orcid.org/0000-0002-4755-1569
Zhengcheng Zhang https://orcid.org/0000-0002-0467-5801

References

1. M. D. Slater, D. Kim, E. Lee, and C. S. Johnson, "Sodium-ion batteries." *Adv. Funct. Mater.*, **23**, 947 (2012).
2. Z. Li, Y. Zhang, and Y. Wang, "High-power and low-cost sodium-ion batteries with a wide operation temperature from −70 °C to 130 °C." *SmartMat*, **4** (2023).
3. C. Che, F. Wu, Y. Li, Y. Li, S. Li, C. Wu, and Y. Bai, "Challenges and breakthroughs in enhancing temperature tolerance of sodium-ion batteries." *Adv. Mater.*, **36**, 2402291 (2024).
4. X. Yin, Z. Lu, J. Wang, X. Feng, S. Roy, X. Liu, Y. Yang, Y. Zhao, and J. Zhang, "Enabling fast Na+ transfer kinetics in the whole-voltage-region of hard-carbon anodes for ultrahigh-rate sodium storage." *Adv. Mater.*, **34** (2022).
5. P. Desai, J. Huang, D. Foix, J.-M. Tarascon, and S. Mariyappan, "Zero volt storage of Na-ion batteries: performance dependence on cell chemistry!." *J. Power Sources*, **551** (2022).
6. C. Yang, S. Xin, L. Mai, and Y. You, "Materials design for high-safety sodium-ion battery." *Adv. Energy Mater.*, **11**(2), 2000974 (2020).
7. Z. Dai, U. Mani, H. T. Tan, and Q. Yan, "Advanced cathode materials for sodium-ion batteries: what determines our choices?" *Small Methods*, **1** (2017).
8. X. Wang et al., "Ultra-stable all-solid-state sodium metal batteries enabled by perfluoropolyether-based electrolytes." *Nat. Mater.*, **21**, 1057 (2022).
9. L. Zhao, T. Zhang, W. Li, T. Li, L. Zhang, X. Zhang, and Z. Wang, "Engineering of sodium-ion batteries: opportunities and challenges." *Engineering*, **24**, 172 (2021).
10. Y. Wan, B. Huang, W. Liu, D. Chao, Y. Wang, and W. Li, "Fast-charging anode materials for sodium-ion batteries." *Adv. Mater.*, **36** (2024).
11. K. Vignaroobanm, R. Kushagra, A. Elango, P. Badami, B.-E. Mellander, X. Xu, T. G. Tucker, C. Nam, and A. M. Kannan, "Current trends and future challenges of electrolytes for sodium-ion batteries." *Int. J. Hydrogen Energy*, **41**, 2829 (2016).
12. Z. Tian, Y. Zou, G. Liu, Y. Wang, J. Yin, J. Ming, and H. N. Alshareef, "Electrolyte solvation structure design for sodium ion batteries." *Adv. Sci.*, **9** (2022).
13. Y. Li, F. Wu, Y. Li, M. Liu, X. Feng, Y. Bai, and C. Wu, "Ether-based electrolytes for sodium ion batteries." *Chem. Soc. Rev.*, **51**, 4484 (2022).
14. Y. Liu, Y. Gong, K. Chen, L. Zhu, Y. An, K. I. Ozoemena, W. Hua, M. Yang, and Q. Pang, "Long-life high-voltage sodium-ion batteries enabled by electrolytes with cooperative Na^+-Solvation." *Adv. Funct. Mater.*, **34** (2024).
15. Y. Jin et al., "Low-solvation electrolytes for high-voltage sodium-ion batteries." *Nat. Energy*, **7**, 718 (2022).
16. X. Xiang, K. Zhang, and J. Chen, "Recent advances and prospects of cathode materials for sodium-ion batteries." *Adv. Mater.*, **27** (2015).
17. M. He, X. Li, J. Wu, and J. Zhu, "Review of cathode materials for sodium-ion batteries." *Prog. Solid State Chem.*, **74** (2024).
18. , X. L. Xiao, K. Tang, D. Wang, M. Long, H. Gao, W. Chen, C. Liu, H. Liu, and G. Wang, "Recent progress of emerging cathode materials for sodium ion batteries." *Mater. Chem. Front.* (2021).
19. Y.-B. Niu, Y.-J. Guo, Y.-X. Yin, S.-Y. Zhang, T. Wang, P. Wang, S. Xin, and Y.-G. Guo, "High-efficiency cathode sodium compensation for sodium-ion batteries." *Adv. Mater.*, **32** (2020).
20. H. Hou, X. Qiu, W. Wei, Y. Zhang, and X. Ji, "Carbon anode materials for advanced sodium-ion batteries." *Adv. Energy Mater.*, **7** (2017).
21. Y. Wen, K. He, Y. Zhu, F. Han, Y. Xu, I. Matsuda, Y. Ishii, J. Cumings, and C. Wang, "Expanded graphite as superior anode for sodium-ion batteries." *Nat. Commun.*, **5**, 4033 (2014).
22. H. He, D. Sun, Y. Tang, H. Wang, and M. Shao, "Understanding and improving the initial Coulombic efficiency of high-capacity anode materials for practical sodium ion batteries." *Energy Storage Mater.*, **23**, 233 (2019).
23. W. Zhang, F. Zhang, F. Ming, and H. N. Alshareef, "Sodium-ion battery anodes: Status and future trends." *EnergyChem*, **1** (2019).
24. D. Djian, F. Alloin, S. Martinet, H. Lignier, and J. Y. Sanchez, "Lithium-ion batteries with high charge rate capacity: influence of the porous separator." *J. Power Sources*, **172**, 416 (2007).
25. Q. Chen, W. Zhuang, Z. Hou, Y. Jiang, J. Wan, T. Zhang, Y. Zhao, and L. Huang, "A dual-function additive to regulate nucleation behavior and interfacial chemistry for ultra-stable Na metal anodes beyond one year." *Adv. Funct. Mater.*, **33**, 2210206 (2022).

26. T. Zhang, L. Yang, X. Yan, and X. Ding, "Recent advances of cellulose-based materials and their promising application in sodium-ion batteries and capacitors." *Small*, **14** (2018).
27. J. Wang, Z. Xu, Q. Zhang, X. Song, X. Lu, Z. Zhang, A. J. Onyianta, M. Wang, M.-M. Titirici, and S. J. Eichhorn, "Stable sodium-metal batteries in carbonate electrolytes achieved by bifunctional, sustainable separators with tailored alignment." *Adv. Mater.*, **34** (2022).
28. F. Wu, N. Zhu, Y. Bai, Y. Li, Z. Wang, Q. Ni, H. Wang, and C. Wu, "Unveil the mechanism of solid electrolyte interphase on Na3V2(PO4)3 formed by a novel NaPF6/BMITFSI ionic liquid electrolyte." *Nano Energy*, **51**, 524 (2018).
29. M. Law, V. Ramar, and P. Balaya, "Na_2MnSiO_4 as an attractive high capacity cathode material for sodium-ion battery." *J. Power Sources*, **359**, 277 (2017).
30. D. Luo, J. Xu, Q. Guo, L. Fang, X. Zhu, Q. Xia, and H. Xia, "Surface-dominated sodium storage towards high capacity and ultrastable anode material for sodium-ion batteries." *Adv. Funct. Mater.*, **28** (2018).
31. J. Zheng, X. Liu, Y. Duan, L. Chen, X. Zhang, X. Feng, W. Chen, and Y. Zhao, "Stable cross-linked gel terpolymer electrolyte containing methyl phosphonate for sodium ion batteries." *J. Membr. Sci.*, **583**, 163 (2019).
32. H. Gao, B. Guo, J. Song, K. S. Park, and J. B. Goodenough, "A composite gel–polymer/glass–fiber electrolyte for sodium-ion batteries." *Adv. Energy Mater.*, **5** (2015).
33. S. Das and V. Adyam, "Optimizing structural and cycling stability in sodium-ion batteries using tailored glass fiber separators." *J. Appl. Electrochem.*, **55**, 619 (2024).
34. X. Li, J. Zhang, X. Guo, C. Peng, K. Song, Z. Zhang, L. Ding, C. Liu, W. Chen, and S. Dou, "An ultrathin nonporous polymer separator regulates Na transfer toward dendrite-free sodium storage batteries." *Adv. Mater.*, **35** (2023).
35. W. Bai, J. Zhu, Y. Wang, M. Xu, and J. Jiang, "Achieving highly stable sodium metal batteries with self-adapting and high-ionic-mobility ceramic fiber membranes." *J. Colloid Interface Sci.*, **660**, 393 (2024).
36. J. I. L. Kim, Y. Choi, K. Y. Chung, and J. H. Park, "A structurable gel-polymer electrolyte for sodium ion batteries." *Adv. Funct. Mater.*, **27** (2017).
37. Z. Liu, G. Li, Q. Qin, L. Mi, G. Li, G. Zheng, C. Liu, Q. Li, and X. Liu, "Electrospun PVDF/PAN membrane for pressure sensor and sodium-ion battery separator." *Advanced Composites and Hybrid Materials*, **4**, 1215 (2021).
38. S. Janakiraman, M. Khalifa, R. Biswal, S. Ghosh, S. Anandhan, and A. Venimadhav, "High performance electrospun nanofiber coated polypropylene membrane as a separator for sodium ion batteries." *J. Power Sources*, **460** (2020).
39. S. Janakiraman, A. Surendran, S. Ghosh, S. Anandhan, and A. Venimadhav, "Electroactive poly(vinylidene fluoride) fluoride separator for sodium ion battery with high coulombic efficiency." *Solid State Ionics*, **292**, 130 (2016).
40. B. Halder, M. G. Mohamed, S.-W. Kuo, and P. Elumalai, "Review on composite polymer electrolyte using PVDF-HFP for solid-state lithium-ion battery." *Materials Today Chemistry*, **36** (2024).
41. C. Likitaporn, M. Okhawilai, P. Kasemsiri, J. Qin, P. Potiyaraj, and H. Uyama, "High electrolyte uptake of MXene integrated membrane separators for Zn-ion batteries." *Sci. Rep.*, **12** (2022).
42. D. L. K. Williams, A. T., M. A. Amann, M. B. Hausinger, M. M. Konarik, and E. I. Nesselrode, "Computerised measurement of contact angles." *Galvanotechnik* (2010).
43. J. E. Tsuchida, F. A. Ferri, P. S. Pizani, A. C. Martins Rodrigues, S. Kundu, J. F. Schneiderce, and E. D. Zanotto, "Ionic conductivity and mixed-ion effect in mixed alkali metaphosphate glasses." *Phys. Chem. Chem. Phys.*, **19**, 6594 (2017).
44. M. T. Hossain, M. A. Shahid, N. Mahmud, A. Habib, M. M. Rana, S. A. Khan, and M. D. Hossain, "Research and application of polypropylene: a review." *Discover Nano*, **19** (2024).
45. D. M. D. Babiker, Z. R. Usha, C. Wan, M. M. E. L. Hassaan, X. Chen, and L. Li, "Recent progress of composite polyethylene separators for lithium/sodium batteries." *J. Power Sources*, **564** (2023).
46. R. Dallaev, T. Pisarenko, D. Sobola, F. Orudzhev, S. Ramazanov, and T. Trčka, "Brief review of PVDF properties and applications potential." *Polymers*, **14**, 4793 (2022).
47. H. Liu, B. Du, M. Xiao, Z. Ran, and Y. Ma, "Dielectric properties of polymer films in strong electromagnetic field for energy storage capacitor." *IEEE Trans. Dielectr. Electr. Insul.*, **29**, 1745 (2022).
48. G. Yi, C. Xu, W. Liu, D. Qu, H. Wang, and H. Tang, "Thermal stability and electrochemical properties of separators for lithium-ion batteries." *Journal of Wuhan University of Technology - Materials Science*, **38**, 1231 (2023).
49. C. Man et al., "Enhanced wetting properties of a polypropylene separator for a lithium-ion battery by hyperthermal hydrogen induced cross-linking of poly (ethylene oxide)." *J. Mater. Chem. A*, **2**, 11980 (2014).
50. J. Wang, J. S., J. Shi, Y. Li, J. You, and F. Bian, "Crystallization-templated high-performance PVDF separator used in lithium-ion batteries." *J. Membr. Sci.*, **670** (2023).
51. I. Mohammad, L. D. J. B., V. Stolojan, C. Crean, and R. C. T. Slade, "Electrospun polar-nanofiber PVDF separator for lithium–sulfur batteries with enhanced charge storage capacity and cycling durability." *Energy Advances*, **3**, 625 (2024).
52. M. Pigłowska, B. Kurc, M. Galiński, P. Fuć, M. Kamińska, N. Szymlet, and P. Daszkiewicz, "Challenges for safe electrolytes applied in lithium-ion cells—A review." *Materials*, **14**, 6783 (2021).
53. A. Rawal, P. V. Kameswara Rao, V. Kumar, and A. Kukovecz, "A critical review on the absorptive glass mat (AGM) separators synergistically designed via fiber and structural parameters." *J. Power Sources*, **430**, 175 (2019).
54. F. Xie, Z. Xu, Z. Guo, and M.-M. Titirici, "Hard carbons for sodium-ion batteries and beyond." *Progress in Energy*, **2** (2020).
55. H. M. Law, J. Yu, S. C. T. Kwok, G. Zhou, M. J. Robson, J. Wu, and F. Ciucci, "A hybrid dual-salt polymer electrolyte for sodium metal batteries with stable room temperature cycling performance." *Energy Storage Mater.*, **46**, 182 (2022).